The alpha-effect in a turbulent liquid-metal plane Couette flow

G. Rüdiger
*Leibniz-Institut für Astrophysik Potsdam, An der Sternwarte 16, D-14482 Potsdam, Germany and Helmholtz-Zentrum Dresden-Rossendorf, P.O. Box 510119, D-01314 Dresden, Germany**

A. Brandenburg
Nordita, AlbaNova University Center, Roslagstullsbacken 23, SE-10691 Stockholm, Sweden and Department of Astronomy, Stockholm University, SE-10691 Stockholm, Sweden

(Dated: January 4, 2012)

The electromotive force in a plane Couette flow of conducting fluids under the influence of a large-scale magnetic field is calculated for driven turbulence. In case of a vertically stratified intensity of the turbulence the resulting α-tensor in presence of a horizontal shear also possesses diagonal elements known as the so-called α-effect. The possibility to measure these components is probed by both quasilinear theory and nonlinear numerical simulations. For all magnetic Prandtl numbers $\lesssim 1$ we find the α-component along the flow in the high-conductivity limit exceeding the other components. In this limit the α's run linear with the magnetic Reynolds number Rm while in the low-conductivity limit they run with the product $\mathrm{Rm}\cdot\mathrm{Re}$. For the small magnetic Prandtl numbers of liquid sodium a value for the electromotive force across the channel of order 0.05...0.5 mV for magnetic fields of about 1 kGauss and velocity fluctuations of about 1 m/s is found for a channel of (say) 50 cm height independent of its width. Such values should be appropriate to be realized in a future laboratory experiment.

PACS numbers: 47.27.Pa, 47.65.+a, 95.30.Qd

arXiv:1201.0652v1 [astro-ph.SR] 3 Jan 2012

I. INTRODUCTION

The electrodynamics in turbulent conducting fluids provides the standard explanation of the existence of magnetic fields of the cosmic objects. The excitation of fields results from the interplay of two different elementary processes. It is known that the turbulent motions are reducing large-scale electrical currents by inducing an electromotive force (EMF) opposite to the direction of the current. One can write

$$\bar{\boldsymbol{\mathcal{E}}} = \overline{\boldsymbol{u}\times\boldsymbol{b}} = -\mu_0\eta_{\rm T}\bar{\boldsymbol{J}}, \qquad (1)$$

where $\eta_{\rm T}$ is the turbulent magnetic diffusivity. In stellar convection zones its value exceeds the molecular (or 'microscopic') value of the magnetic resistivity by many orders of magnitudes.

In this paper the EMF is derived for a turbulent fluid in the presence of a shear flow $\boldsymbol{U}$ and a uniform background field $\boldsymbol{B}$. The fluctuating flow components are denoted by $\boldsymbol{u}$ and the fluctuating field components are denoted by $\boldsymbol{b}$.

For a turbulent dynamo the enhanced dissipation must be overcome by an induction process which does not run with the electric current. One also knows that under the influence of global rotation and a uniform magnetic field, anisotropic turbulence produces an EMF parallel to the field, i.e.

$$\bar{\boldsymbol{\mathcal{E}}} = \alpha\bar{\boldsymbol{B}} - \ldots. \qquad (2)$$

Here, α is a pseudo-scalar formed by the rotation vector $\boldsymbol{\Omega}$ and the anisotropy direction $\boldsymbol{g}$ with $\alpha \propto \boldsymbol{g}\cdot\boldsymbol{\Omega}$. Often as the anisotropy direction is the gradient of the density stratification in the fluid is used, but it is also possible that an intensity gradient close to rigid boundaries forms the preferred direction.

The resulting dynamo equation in rotating and stratified plasma is

$$\frac{\partial\bar{\boldsymbol{B}}}{\partial t} = \mathrm{rot}\Big(\alpha\bar{\boldsymbol{B}} - (\eta+\eta_{\rm T})\mathrm{rot}\bar{\boldsymbol{B}}\Big), \qquad (3)$$

which indeed has non-decaying solutions if the α-effect exceeds a critical value ('α^2-dynamo').

In many of papers the presented concept of a turbulent dynamo has been applied to planets, stars, accretion disks, galaxies and galaxy clusters (many references given by [1]. Only very few papers, however, deal with an experimental confirmation of the validity of relations (1) and (2) in the laboratory. This is surprising insofar as Eq. (3) as a simple consequence of Eqs. (1) and (2) seems to summarize all our knowledge about the electrodynamics in rotating turbulent fluid conductors. Generally, the validity of Eq. (1) is not seriously doubted. However, the existing laboratory experiments report an increase of the molecular value of η by only a few percent. This is a surprising situation as the eddy-concept of the effective dissipation in turbulent media governs much of the cosmical physics from the climate research, geophysics up to the theory of star formation and quasars.

An even more dramatic situation holds with respect to the α-effect. There are one or two existing experiments on the basis of the idea that the α-effect is essentially a measure of the swirl of the fluid. It has indeed been

*Electronic address: gruediger@aip.de

shown that a fluid with imposed helicity (imposed by rigid, swirling channels), produces an EMF in the direction of an imposed field; see [2–4]. It is not yet shown, however, that a rotating fluid with helicity which is *not* imposed (but results from the global rotation of the fluid) leads to an observable α-effect. In nature, helicity is usually due to the interaction of rotating turbulence with density stratification. The present proposal also aims in the direction to probe the possibilities of such a more rigorous α-effect experiment. The many difficulties for such an experiment which we shall demonstrate make it understandable that an experiment without prescribed helicity not yet exists in the theory and in the MHD laboratory.

It is easy to formulate the overall problem of all α-effect experiments. With Eq. (2) the potential difference between the endplates of the container in direction of the mean magnetic fields is

$$\Delta\Phi = \alpha_{\rm dyn} B H \tag{4}$$

with H as the distance between the endplates. Hence for (say) $H \simeq 100$ cm and (say) $B \simeq 1000$ Gauss the potential difference is $\Delta\Phi = |\alpha_{\rm dyn}|$ in mV and cm/s, respectively. The maximum α-value is of the order $u_{\rm rms}$ hence $\Delta\Phi \lesssim u_{\rm rms}$ in mV. For $u_{\rm rms} \simeq 1$ cm/s the induced potential difference, therefore, is maximally 1 mV. A container of 5 cm radius rotating with 1 Hz has a linear outer velocity of more than 30 cm/s so that $u_{\rm rms} \simeq 1$ cm/s might be considered as a conservative estimate. We find as a necessary condition for any α-experiment that one must be able to measure potential differences *smaller* than a few mV. The α-experiment in Riga worked with $B \simeq 1$ kGauss and velocities of order m/s so that the $\Delta\Phi$ exceeded 10 mV. This experiment, however, used a prescribed helical geometry to mimic the symmetry breaking between left and right helicity [2].

If the basic rotation is not uniform then its shear induces toroidal magnetic fields so that for sufficiently strong shear even the α-effect can be rather small ('$\alpha\Omega$-dynamo'). Also turbulence subject to a plane shear flow (without rotation!) of a liquid metal is able to work as a dynamo if the turbulence intensity is stratified in the direction(orthogonal to the shear flow plane, see [5].A basic rotation may thus not be the only flow system whose influence enables the turbulence to generate global fields.

In the present paper a plane Couette flow is considered to analyze the characteristic issues of the corresponding α effect and to design a possible experiment to measure its amplitude.

II. THE MEAN ELECTROMOTIVE FORCE

Consider a plane shear flow with uniform vorticity in the vertical z direction, i.e.

$$\bar{U}_y = Sx. \tag{5}$$

The shear flow may exist in a turbulence field which does not possess any other anisotropy than that induced by the shear (5) itself. The one-point correlation tensor is

$$Q_{ij} = \overline{u_i(\boldsymbol{x},t) u_j(\boldsymbol{x},t)}. \tag{6}$$

The correlation tensor may be constructed by a perturbation method. The fluctuating velocity field is represented by a series expansion,

$$\boldsymbol{u} = \boldsymbol{u}^{(0)} + \boldsymbol{u}^{(1)} + \boldsymbol{u}^{(2)} + \dots\,, \tag{7}$$

where the upper index shows the order of the contributions in terms of the mean shear flow.

The zero-order term represents the 'original' isotropic turbulence which is assumed as not yet influenced by the shear. The spectral tensor for the original turbulence is

$$\hat{Q}_{ij}^{(0)} = \frac{E(k,\omega)}{16\pi k^2}\left(\delta_{ij} - \frac{k_i k_j}{k^2}\right), \tag{8}$$

where the positive-definite spectrum E gives the intensity of isotropic fluctuations, i.e.

$$\overline{\boldsymbol{u}^{(0)^2}} = \int_0^\infty\!\!\int_0^\infty E(k,\omega)\ {\rm d}k\ {\rm d}\omega. \tag{9}$$

For analytical calculations the one-parametric spectrum

$$E(k,\omega) = \frac{2}{\pi}\frac{w}{\omega^2 + w^2}\hat{E}(k), \tag{10}$$

can be used which provides $E \propto \delta(\omega)$ in the limit of $w \to 0$ and leads to white noise for large w. The correlation time of the turbulence is defined by $\tau_{\rm corr} = 1/w$.

By definition, the magnetic-diffusivity tensor relates the mean electromotive force (1) to the gradients of the mean magnetic field via the relation $\bar{\mathcal{E}}_i = \eta_{ijk}\bar{B}_{j,k}$. This tensor for an isotropic turbulence influenced by a mean field shear flow (5) has been constructed up to the first order in the shear [5], [6]. It has been shown that the combination of the shear and the shear-induced parts of the magnetic-diffusion tensor are not able to operate as a dynamo.

It has also been shown that the shear in combination with a *stratified* turbulence provides a helical turbulence which leads in Eq. (2) to an α-effect [5]. Here α must be a pseudotensor so that an ϵ-tensor has to appear in the α-coefficients. The construction of the EMF $\bar{\mathcal{E}}_i = \epsilon_{ijk}\overline{u_j b_k}$ is the only possibility for the ϵ-tensor to appear. Therefore, the subscript of $\mathcal{E}_i$ is always a subscript of the ϵ-tensor. As the ϵ-tensor is of 3rd rank an inhomogeneity of turbulence with the stratification vector, $\boldsymbol{g} = \boldsymbol{\nabla}\log u_{\rm rms}^2$ with $u_{\rm rms} = \sqrt{\overline{u^2}}$, must also be present for the α-effect to exist. If the shear flow is included to its first order, the general structure of the α-tensor is

$$\begin{aligned}\alpha_{ij} &= \gamma\epsilon_{ijk}g_k + \left(\alpha_1\epsilon_{ikl}\bar{U}_{j,k} + \alpha_2\epsilon_{ikl}\bar{U}_{k,j}\right)g_l + \\ &+ \alpha_3\epsilon_{ikl}g_j\bar{U}_{l,k} + \alpha_4\epsilon_{ikj}\bar{U}_{l,k}g_l + \alpha_5\epsilon_{ijk}\bar{U}_{k,l}g_l.\end{aligned} \tag{11}$$

If the stratification is along the vertical z-axis it follows from (11) that

$$\begin{aligned}\alpha_{xx} &= \alpha_2 g_z S = \alpha_x S,\\ \alpha_{yy} &= -\alpha_1 g_z S = \alpha_y S,\\ \alpha_{zz} &= \alpha_3 g_z S = \alpha_z S\\ \alpha_{xy} &= -\alpha_{yx} = \gamma g_z = \Gamma. \end{aligned} \tag{12}$$

The turbulent pumping is described by α_{xy}. The anisotropy of the α-tensor is described by the difference between α_x and α_y. In the used geometry the α_{yy} (i.e. the coefficient α_1 defined below) plays the main role in all cosmical applications while in the proposed experiment in a turbulent shear flow the coefficient α_2 is probed which produces the EMF perpendicular to the flow.

The coefficients of (11) read

$$\gamma = \frac{1}{6}\int_0^\infty\int_0^\infty \frac{\eta k^2 E(k,\omega)}{\omega^2+\eta^2 k^4}\mathrm{d}k\ \mathrm{d}\omega \tag{13}$$

for the pumping term and

$$\alpha_n = \int_0^\infty\int_0^\infty A_n E\left(k,\omega\right)\mathrm{d}k\ \mathrm{d}\omega, \quad n=1,2,...5, \tag{14}$$

for the α-effect with

$$\begin{aligned} A_1 &= \frac{4\nu\eta^3 k^8 + 2\omega^2\eta\left(\nu+\eta\right)k^4}{15\left(\omega^2+\nu^2k^4\right)\left(\omega^2+\eta^2k^4\right)^2} +\\ &+ \frac{\eta^2k^4\left(\eta^2k^4-3\omega^2\right)}{15\left(\omega^2+\eta^2k^4\right)^3},\\ A_2 &= -\frac{\eta^2\nu^3\left(4\eta-5\nu\right)k^{12}}{60\left(\omega^2+\nu^2k^4\right)^2\left(\omega^2+\eta^2k^4\right)^2} -\\ &- \frac{\omega^2\nu\left(28\eta^3-4\eta^2\nu+12\eta\nu^2+5\nu^3\right)k^8}{60\left(\omega^2+\nu^2k^4\right)^2\left(\omega^2+\eta^2k^4\right)^2} -\\ &- \frac{\omega^4\eta\left(\eta+36\nu\right)k^4-5\omega^6}{60\left(\omega^2+\nu^2k^4\right)^2\left(\omega^2+\eta^2k^4\right)^2}\\ A_3 &= -\frac{8\omega^2k^4(\omega^2+\nu\eta k^4)\eta(\nu+\eta)}{30(\omega^2+\nu^2k^4)^2(\omega^2+\eta^2k^4)^2} -\\ &- \frac{3\eta^4k^8-24\omega^2\eta^2k^4+5\omega^4}{30(\omega^2+\eta^2k^4)^3} \end{aligned} \tag{15}$$

for the kernels. Only the terms occurring in (12) have been given. Note that A_3 for $\nu\to 0$ exists

$$A_3 = -\frac{11\eta^4k^8-16\omega^2\eta^2k^4+5\omega^4}{30(\omega^2+\eta^2k^4)^3}. \tag{16}$$

For small Pm the expression for A_1 simplifies to

$$\begin{aligned} A_1 &= \frac{1}{15}\frac{1}{\left(\omega^2+\eta^2k^4\right)^2}\left\{\frac{4\nu\eta^3k^8}{\omega^2+\nu^2k4}+\right.\\ &\left.+\ \frac{\eta^2k^4\left(3\eta^2k^4-\omega^2\right)}{\omega^2+\eta^2k^4}\right\}. \end{aligned} \tag{17}$$

The first expression on the RHS for $\nu\to 0$ forms a δ-function, so that

$$\begin{aligned}\alpha_1 &= \frac{2\pi}{15w}\int_0^\infty\frac{E(k,0)}{\eta k^2}\mathrm{d}k+\ldots\\ &\simeq \frac{2\pi}{15}\mathrm{Rm}\ \ell_{\mathrm{corr}}^2+\ldots\end{aligned} \tag{18}$$

with

$$\mathrm{Rm} = \frac{u_{\mathrm{rms}}^2\tau_{\mathrm{corr}}}{\eta}\simeq\frac{3\eta_{\mathrm{T}}}{\eta}. \tag{19}$$

The missing terms in (18) result to be of the same order.

The white-noise approximation mimics the high-conductivity limit which holds for cosmical applications. In this approach the spectrum does not depend on the frequency ω up to a maximum value $\omega_{\max}$ from which one the power spectrum vanishes. It is a turbulence model with very short correlation time, i.e. $\tau_{\mathrm{corr}}\simeq 1/\omega_{\max}$. One finds from (17) after integration

$$\alpha_1 = \frac{\pi}{6\eta}\int_0^\infty\frac{E(k,0)}{k^2}\mathrm{d}k. \tag{20}$$

The resulting integral can be written as $\tau_{\mathrm{corr}}\ell_{\mathrm{corr}}^2u_{\mathrm{rms}}^2$ so that

$$\alpha_1 = \frac{\pi}{6}\mathrm{Rm}\ \ell_{\mathrm{corr}}^2, \tag{21}$$

which hardly differs from the result (18). As it must the factor $\pi/6$ also appears in Fig. 1 (middle, bottom) as the value of I_1 for $\tau=0$. For $\mathrm{Pm}=1$ the corresponding expression is

$$\alpha_1 = \frac{\pi}{15}\mathrm{Rm}\ \ell_{\mathrm{corr}}^2. \tag{22}$$

Note that the value for small Pm exceeds the value for $\mathrm{Pm}=1$. For given η smaller ν lead to *higher values* of the EMF.

The full expression might be written in the form

$$\alpha_1 \simeq I_1\ \mathrm{Rm}\ \ell_{\mathrm{corr}}^2, \tag{23}$$

where I_1 is numerically given in Fig. 1. It is the result of a numerical integration under use of a spectral function of the form $\exp(-\tau^2\omega^2)$ with the dimensionless parameter

$$\tau = \eta k^2\tau_{\mathrm{corr}}\simeq 1/\mathrm{Rm}. \tag{24}$$

While small τ represent the high-conductivity limit the larger τ represent the low-conductivity limit. Obviously, the high-conductivity limit can be modeled with a white-noise spectrum (Eq. (10) with $w\to\infty$) while the low-conductivity limit can be treated by use of the δ-function (Eq. (10) with $w\to 0$). It follows from $(15)_1$

$$\alpha_1 = \frac{1}{15}\left(1+\frac{4}{\mathrm{Pm}}\right)\mathrm{Rm}^2\ \ell_{\mathrm{corr}}^2, \tag{25}$$

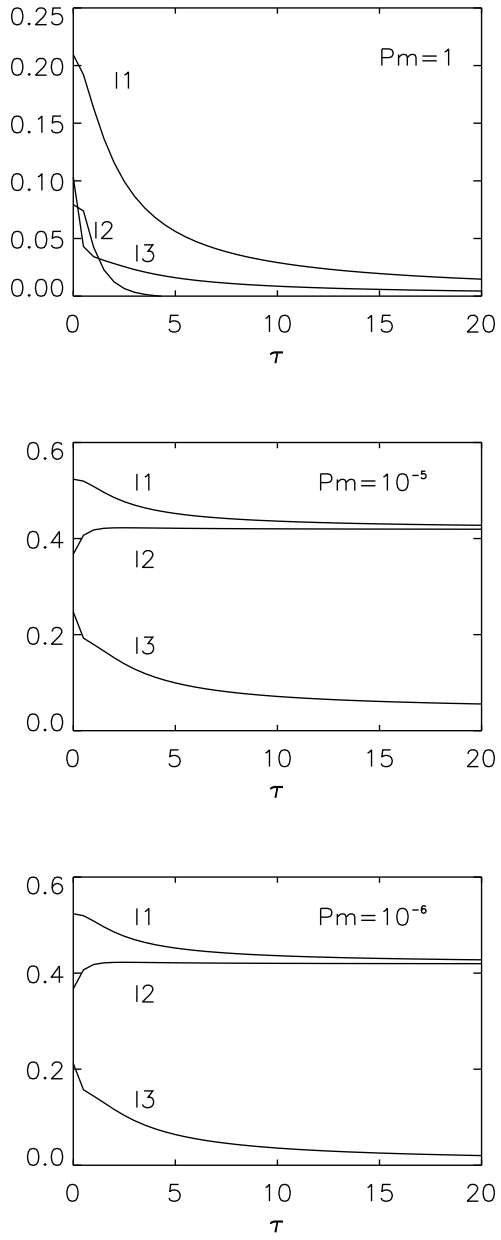

FIG. 1: The numerical values of the coefficients I_1, I_2 and I_3. Top: Pm = 1, middle: Pm = 10^{-5}, bottom: Pm = 10^{-6}. Note that in the high-conductivity limit ($\tau \to 0$, white noise spectrum) the coefficients I_1 and I_2 for Pm $\ll 1$ exceed the values for Pm = 1. Laboratory experiments with turbulent flows of liquid metals work with $\tau \simeq 1...10$.

so that Pm = 1 leads to $\alpha_1 = \frac{1}{3}\mathrm{Rm}^2\ \ell^2_{\rm corr}$ and for small magnetic Prandtl number one finds $\alpha_1 = \frac{4}{15}\mathrm{Re\ Rm}\ \ell^2_{\rm corr}$, with Re = Rm/Pm as the Reynolds number. Hence, in the low-conductivity (small Rm) limit the α effect runs with Re $\cdot$ Rm while in the high-conductivity limit (large Rm) the α effect runs with Rm. Very similar expressions also occur if the shear flow is formally replaced by a basic rotation (Rüdiger 1978).

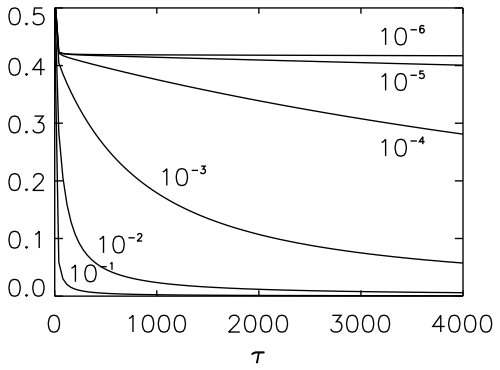

FIG. 2: I_1 for various Pm. Note that for given magnetic diffusivity η fluids with much smaller viscosity (like sodium and gallium) are even better qualified for laboratory experiments.

Figure 2 demonstrates the behavior of the numerical integrals for decreasing Pm and growing τ. The integrals are running with $(1+\mathrm{Pm}\ \tau)^{-1}$ so that for Pm $\tau \gg 1$ the relation $\alpha_1 \propto$ Re Rm indeed results. Again, for given magnetic diffusivity smaller values of the viscosity enhance (!) the resulting α-effect.

In experiments with liquid metals the Rm is of order 0.1...1 so that $\tau \simeq 1...10$. In this domain and for small Pm the coefficient I_1 hardly changes with τ (see Fig. 1). Its approximate value is 0.5 which is very close to the value $\pi/6$ valid in the high-conductivity limit. The reason is that for small Pm the transition of I_1 to the low-conductivity limit only happens at rather high values of τ (Fig. 2).

Similar calculations for α_2 lead to $\alpha_2 \simeq -I_2\ \mathrm{Rm}\ \ell^2_{\rm corr}$, with I_2 also plotted in Fig. 1. For medium τ and small Pm we find $I_2 \simeq I_1$, i.e.

$$\alpha_2 \simeq -0.5\ \mathrm{Rm}\ \ell^2_{\rm corr}. \tag{26}$$

In the low-conductivity limit we have

$$\alpha_2 = -\frac{1}{60}\left(\frac{4}{\mathrm{Pm}} - 5\right)\mathrm{Rm}^2\ \ell^2_{\rm corr}, \tag{27}$$

which changes its sign at Pm = 0.8. For small Pm it can also be written as

$$\alpha_2 = -\frac{1}{15}\mathrm{RmRe}\ \ell^2_{\rm corr}, \tag{28}$$

In summary, the plots in Fig. 1 reveal an important influence of the viscosity value for given diffusivity value. For small Pm in the low-conductivity limit the ratio of I_2 to I_1 approaches unity while it is very small for Pm = 1. The magnetic Prandtl number is highly different for liquid metal and for numerical simulations. Figure 1 shows that in numerical simulations the α_{xx} should be much smaller than the α_{yy} what is not true for laboratory conditions with their small Pm.

The α_3 yields $\alpha_3 \simeq -I_3$ Rm $\ell_{\rm corr}^2$ with I_3 of about 0.1 for small Pm (see Fig. 1). The horizontal components of the α-tensor are thus of the same order of magnitude but the vertical component appears to be smaller. Note that for Pm = 1 the α_1 strongly exceeds the α_2 but it does not for small Pm. The signs of all components are identical.

The pumping term does not depend on the shear. After (13) for small η it does not run with $1/\eta$, so that it is simply

$$\gamma \simeq \langle u'^2 \rangle \tau_{\rm corr} \simeq \eta \ {\rm Rm}. \tag{29}$$

It can only be measured if the external field B_0 lies in the shear plane.

III. NUMERICAL SIMULATIONS

It is straightforward to verify the existence of an α-effect using numerical simulations of non-uniformly forced turbulent shear flows in Cartesian coordinates. We perform simulations in a cubic domain of size L^3, so the minimal wavenumber is $k \equiv k_1 = 2\pi/L$. We solve the governing equations of compressible hydrodynamics with an isothermal equation of state with constant sound speed $c_{\rm s}$. The set of governing equations is

$$\frac{{\rm D}\boldsymbol{U}}{{\rm D}t} = SU_x \hat{\boldsymbol{y}} - c_{\rm s}^2 \boldsymbol{\nabla} \ln \rho + \boldsymbol{f} + \rho^{-1} \boldsymbol{\nabla} \cdot 2\rho\nu \mathsf{S}, \tag{30}$$

$$\frac{{\rm D} \ln \rho}{{\rm D}t} = -\boldsymbol{\nabla} \cdot \boldsymbol{U}, \tag{31}$$

where ${\rm D}/{\rm D}t = \partial/\partial t + \boldsymbol{U} \cdot \boldsymbol{\nabla} + Sx \ \partial/\partial y$ is the advective derivative with respect to the full velocity field (including the shear flow), $\boldsymbol{U}$ is the departure from the mean shear flow, and $\mathsf{S}_{ij} = \frac{1}{2}(\partial_i U_j + \partial_j U_i) - \frac{1}{3}\delta_{ij} \boldsymbol{\nabla} \cdot \boldsymbol{U}$ is the trace-less rate of strain matrix. The flow is driven by a random forcing function consisting of nonhelical waves with wavenumbers whose modulus lies in a narrow band around an average wave number $k_{\rm f} = 5k_1$ [8]. We arrange the amplitude of the forcing function such that the rms velocity increases with height while the maximum Mach number remains below 0.1, so the effects of compressibility are negligible.

We use the kinematic test-field method [9] in the Cartesian implementation [10] to compute from the simulations simultaneously the relevant components of the α effect and turbulent diffusivity tensors, α_{ij} and η_{ij}, We do this by solving an additional set of equations governing the departure of the magnetic field from a set of given mean fields. This mean field is referred to as the test field and is marked by the superscript T. For each test field $\overline{\boldsymbol{B}}^{\rm T}$, we find a corresponding fluctuation $\boldsymbol{b}^{\rm T} = \boldsymbol{\nabla} \times \boldsymbol{a}^{\rm T}$ by solving the inhomogeneous equation for the corresponding vector potential $\boldsymbol{a}^{\rm T}$,

$$\frac{\mathcal{D}\boldsymbol{a}^{\rm T}}{\mathcal{D}t} = -Sa_y^{\rm T}\hat{\boldsymbol{x}} + \overline{\boldsymbol{U}} \times \boldsymbol{b}^{\rm T} + \boldsymbol{u} \times \overline{\boldsymbol{B}}^{\rm T} + \left(\boldsymbol{u} \times \boldsymbol{b}^{\rm T}\right)' + \eta \nabla^2 \boldsymbol{a}^{\rm T}, \tag{32}$$

where $\mathcal{D}/\mathcal{D}t = \partial/\partial t + Sx \ \partial/\partial y$ is the advective derivative with respect to the imposed shear flow only, and $\left(\boldsymbol{u} \times \boldsymbol{b}^{\rm T}\right)' = \boldsymbol{u} \times \boldsymbol{b}^{\rm T} - \overline{\boldsymbol{u} \times \boldsymbol{b}^{\rm T}}$ is the fluctuating part of $\boldsymbol{u} \times \boldsymbol{b}^{\rm T}$. We compute the corresponding mean electromotive force, $\overline{\boldsymbol{\mathcal{E}}}^{\rm T} = \overline{\boldsymbol{u} \times \boldsymbol{b}^{\rm T}}$, which is then related to $\overline{\boldsymbol{B}}^{\rm T}$ and its curl, $\mu_0 \overline{\boldsymbol{J}}^{\rm T} = \boldsymbol{\nabla} \times \overline{\boldsymbol{B}}^{\rm T}$, via

$$\overline{\mathcal{E}}_i^{\rm T} = \alpha_{ij} \overline{B}_j^{\rm T} - \eta_{ij} \mu_0 \overline{J}_j^{\rm T}. \tag{33}$$

We use 4 different test fields with x or y components being proportional to $\sin kz$ or $\cos kz$. The x and y components of Eq. (33) constitute then 8 equations for the 4 relevant components of $\alpha_{ij}(z,t)$ and $\eta_{ij}(z,t)$.

We adopt periodic boundary conditions in the y direction, shearing–periodic boundary conditions in the x direction, and stress-free perfect conductor boundary conditions in the z direction, i.e.,

$$\partial_z u_x = \partial_z u_y = u_z = a_x^{\rm T} = a_y^{\rm T} = \partial_z a_z^{\rm T} = 0. \tag{34}$$

A numerical resolution of 64^3 mesh points was found to be sufficient. The Pencil Code[18] has been used for all calculations.

Simulations are performed for a number of different parameter combinations. The quantities S and g_z are positive in the calculations presented here, i.e. the basic velocity (5) grows in the positive x direction while the turbulence intensity grows in the positive z direction. To make contact with laboratory experiments, we focus here on the case of low conductivity and choose ${\rm Rm} \equiv u_{\rm rms}/\eta k_{\rm f} = 0.2$, which is consistent with our definition of Eq. (19) with a Strouhal number of unity, i.e., $\tau_{\rm corr} u_{\rm rms} k_{\rm f} = 1$.

As in earlier work using fully helical turbulence, we present the components of α_{ij} and η_{ij} in normalized form in terms of $\alpha_0 = u_{\rm rms}/3$ and $\eta_{\rm T0} = u_{\rm rms}/3k_{\rm f}$, respectively. The shear of the background flow is normalized with the speed of sound, i.e.

$$S = sc_{\rm ac}k_1 = \frac{2\pi s u_{\rm rms}}{{\rm Ma}D} \tag{35}$$

with the Mach number ${\rm Ma} = u_{\rm rms}/c_{\rm ac}$. Here, D $(= L)$ is the distance between the walls, i.e. the width of the domain in the x direction. In the simulations we work with $s = 0.2$ and ${\rm Ma} = 0.05$. Hence,

$$\frac{\alpha_{yy}}{\alpha_0} = -12 \ I_1 \ s \frac{\ell_{\rm corr}^2}{D^2} \ \frac{\rm Rm}{\rm Ma}. \tag{36}$$

Following Eqs. (12), both the streamwise and the spanwise α-tensor components, α_{yy} and α_{xx}, should be negative. As the simulations are done for Pm = 1 the $|\alpha_{yy}|$ should strongly exceed the value of $|\alpha_{xx}|$.

Figure 3a shows these predictions as fulfilled. They hold for Rm = 0.2 and $k_{\rm f}/k_1 = 5$ so that 10 cells exist in the vertical direction. From Eq. (36) one finds $\alpha_{yy}/\alpha_0 \simeq -0.01$. Both the α-tensor components are negative and $|\alpha_{yy}|$ dominates. Its amplitude is indeed 0.01. For Pm =

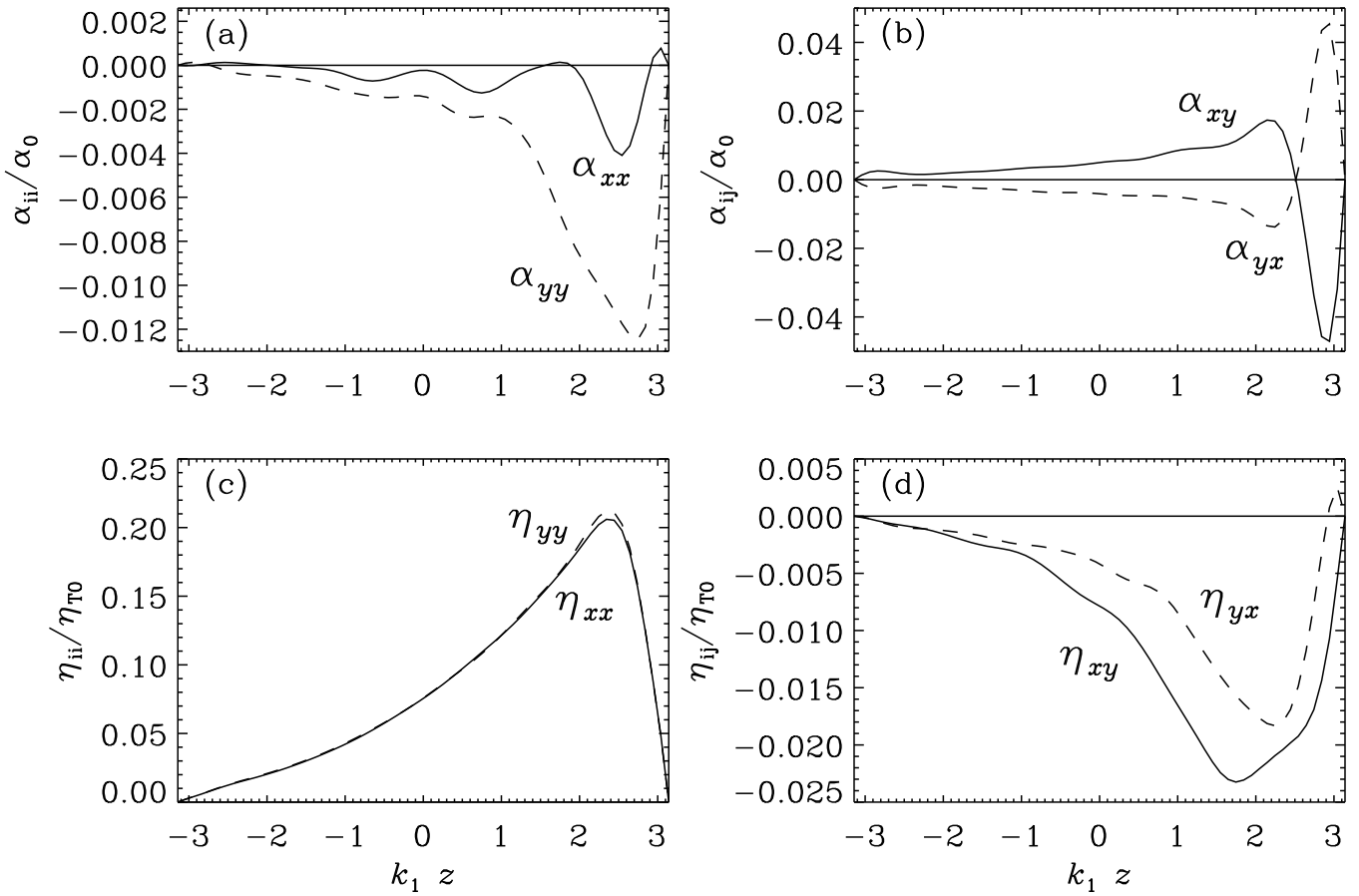

FIG. 3: Simulations with positive shear ($s = 0.2$): The numerical values for α (top) and the two shear–current terms η_{xy} and η_{yx} (bottom).

1 the I_2 is strongly reduced relative to I_1 so that the small amplitude of α_{xx} in Fig. 3a becomes understandable. For small magnetic Prandtl number this reduction does not exist (see Fig. 1). The simulations also confirm that the signs of the diagonal components of the α tensor only depend on the sign of the product $g_z S$, as formulated in the relations (12).

Next, we look at the off-diagonal components of α_{ij}; see Fig. 3b. Note that $\alpha_{yx} \approx -\alpha_{xy}$, which corresponds to a turbulent pumping velocity in the z direction. It is negative for $k_1 z < 2.5$, corresponding to downward transport, i.e., down the gradient of the turbulent intensity, as expected [7]. Near the top of the domain, the gradient of the turbulent intensity is reversed and so is the sign of the pumping velocity, α_{yx}.

IV. SHEAR–CURRENT EFFECTS

Let us now discuss the components of the η_{ij} tensor. Before we turn to the shear–current effect, we note that the two relevant diagonal components are nearly equal, i.e., $\eta_{xx} \approx \eta_{yy}$ (Fig. 3c). This high degree if isotropy of turbulent diffusion in the xy plane has already been in earlier measurements of turbulent diffusivity in turbulent shear flows [10, 11]. The maximum of $\eta_T = (\eta_{xx} + \eta_{yy})/2$ is about 20% of the reference value η_{T0}, which agrees with the fact that for $\mathrm{Rm} \ll 1$, $\eta_T/\eta_{T0} \approx \mathrm{Rm}$ [12].

Let us turn to the off-diagonal components. For non-stratified shear flows one finds

$$\eta_{xy} = \eta_x\ S, \qquad \eta_{yx} = \eta_y\ S, \tag{37}$$

so that the η-terms depend on the sign and the amplitude of S. In a quasilinear theory (SOCA) the η_y proves to be negative-definite [5]. For positive shear the coefficient η_{yx}, therefore, is expected to be negative. This result has also been confirmed for $\mathrm{Rm} \leq 200$ [10]. The possibility of dynamo action in these nonhelical shear flows [10, 13] is therefore not explained by the shear–current effect [14], but instead by the incoherent alpha–shear dynamo [15].

The same dependence of the sign of η_{yx} on that of S holds also for η_{xy}, but only for Pm of order unity and in the low conductivity limit (small Rm). Both the conditions are fulfilled for our simulations. Experiments of liquid metals, however, concern small magnetic Prandtl numbers for which the η_x results as positive. As simulations for such small Pm are not positive, only experiments can finally provide the sign of η_x. The numerical

simulations with positive shear and Pm = 1 indeed produce the expected negative values for both η_{xy} and η_{yx} (Fig. 3d).

V. SHEAR-FLOW ELECTRODYNAMICS

The electromotive force across a channel after (12) is

$$\mathcal{E}_x = \alpha_2 g_z S B_0 \tag{38}$$

so that the potential difference $\delta\Phi_x$ between the walls with their distance D is

$$\begin{aligned}\delta\Phi_x &= \alpha_2 g_z S D B_0 \simeq -0.5\mathrm{Rm}\ell_{\rm corr}^2 g_z U B_0 \\ &\simeq -\mathrm{Rm}\ \lambda^2\ H U B_0 \end{aligned}\tag{39}$$

with $g_z = -2/H$ as the vertical scale height of the turbulence stratification and the ratio $\lambda = \ell_{\rm corr}/H$. The amplitude of the mean shear flow is U. Note that the width D of the channel does not appear in (39). Hence,

$$\delta\Phi_x[\mathrm{mV}] \simeq 10\ \mathrm{Rm}\lambda^2 \left[\frac{H}{10\,\mathrm{cm}}\right]\left[\frac{U}{\mathrm{m/s}}\right]\left[\frac{B_0}{\mathrm{kGauss}}\right] \tag{40}$$

so that with (say) $\lambda \simeq 0.1$ and a channel of 50 cm height, a shear flow of 1 m/s subject to a magnetic field of 1000 Gauss leads to a potential difference of

$$\delta\Phi_x \simeq 0.5\ \mathrm{Rm}\ [\mathrm{mV}]. \tag{41}$$

For the (maximal) value of Rm $\simeq 0.1...1$ ($u_{\rm rms} \simeq 1$m/s and $\ell_{\rm corr} \simeq 5$ cm) the measurements may provide a potential difference of 0.05...0.5 mV. The numbers are quite similar to those of the Riga experiment [2, 7]. The basic difference is that in a shear flow experiment, the helicity is not prescribed but it is naturally produced by the interaction of the (stratified) turbulence with the background shear.

If the external field is *perpendicular* to the shear plane, then the result for the potential difference in the z direction results as

$$\delta\Phi_z \simeq \delta\Phi_x \frac{H}{D}\frac{I_3}{I_2}. \tag{42}$$

After Fig. 1 the ratio I_3/I_2 is of the order of 0.1 so that for $D \simeq H$ the spanwise potential difference is smaller than the same value in the perpendicular x direction. For narrow channels with $D \simeq 0.1H$ both values are the same. Note that the statement bases on the assumption $\ell_{\rm corr}/H \simeq$ const. in both cases. Note also that turbulence which is stratified in the z direction, there is no pumping if also the magnetic field points in the spanwise direction.

VI. CONCLUSIONS

Laboratory studies of homogeneous dynamos are still in their infancy. The only working dynamo where the flow pattern is not stronhgly constrained by pipes or container walls is the experiment in Cadarache [16] where, however, the effects of soft iron play an important and not well understood role. No contact with the α-effect in mean-field theory has been possible in that case. The present proposal of measuring the α-effect in an *unconstrained* turbulent flow would therefore be a major step forward. In such an experiment, the pseudo-scalar necessary for producing helicity comes from the stratification of turbulent intensity giving rise to a polar vector and the vorticity associated with the shear flow giving rise to an axial vector. It has been shown, therefore, that the basic effects of the theory of the turbulent dynamo which are usually considered as special properties of rotating fluids can also be found for the plane-shear flow.

The present work yields a detailed prediction about the sign and magnitude of the tensor components of α_{ij} and η_{ij}. It may motivate the construction of a suitable experiment using liquid metals to achieve a measurable α-effect. The needed vertical stratification of the turbulence intensity must experimentally imitated using grids with nonuniform mesh sizes and/or by walls of increasing/decreasing roughness of the walls in vertical direction.

We have shown that the values of α are small compared with naive estimates. In fact, it may not be possible that such flows could produce a supercritical dynamo in the conceivable future. Nevertheless, even in the subcritical case, an α-effect should be measurable, which would thus open the possibility of detailed comparisons between theory, simulations, and experiments. Once such a comparison is possible, there will be more details that should be investigated. One of them concerns the modifications of the results in the presence of imperfect scale separation in space and time. For oscillatory dynamos, this effect can significantly lower the excitation conditions for the dynamo compared to standard mean-field estimates [17].

[1] G. Rüdiger and R. Hollerbach, *The Magnetic Universe: Geophysical and Astrophysical Dynamo Theory* (Wiley-VCH, Berlin, 2004).

[2] M. Steenbeck, I. M. Kirko, A. Gailitis, A. P. Klawina, F. Krause, I. J. Laumanis, and O. A. Lielausis, Monats. Dt. Akad. Wiss. **9**, 714 (1967).

[3] R. Stepanov, R. Volk, S. Denisov, P. Frick, V. Noskov, and J.-F. Pinton, Phys. Rev. E **73**, 046310 (2006).

[4] P. Frick, S. Denisov, V. Noskov, and R. Stepanov, Astron. Nachr. **329**, 706 (2009).

[5] G. Rüdiger and L. L. Kitchatinov, Astron. Nachr. **327**, 298 (2006).

[6] K.-H. Rädler and R. Stepanov, Phys. Rev. E **73**, 056311 (2006).
[7] F. Krause and K.-H. Rädler, *Mean-Field Magnetohydrodynamics and Dynamo Theory* (Pergamon Press, Oxford, 1980).
[8] N. E. L. Haugen, A. Brandenburg, and W. Dobler, Phys. Rev. E **70**, 016308 (2004).
[9] M. Schrinner, K.-H. Rädler, D. Schmitt, M. Rheinhardt, and U. R. Christensen, Geophys. Astrophys. Fluid Dynam. **101**, 81 (2007).
[10] A. Brandenburg, K.-H. Rädler, M. Rheinhardt, and P.J. Käpylä, Astrophys. J. **676**, 740 (2008).
[11] A. Brandenburg, Astron. Nachr. **326**, 787 (2005).
[12] S. Sur, A. Brandenburg, and K. Subramanian, Mon. Not. R. Astron. Soc. **385**, L15 (2008).
[13] T. A. Yousef, T. Heinemann, A. A. Schekochihin, N. Kleeorin, I. Rogachevskii, A.B. Iskakov, S. C. Cowley, and J. C. McWilliams, Phys. Rev. Lett. **100**, 184501 (2008).
[14] I. Rogachevskii and N. Kleeorin, Phys. Rev. E **68**, 036301 (2003).
[15] E. T. Vishniac and A. Brandenburg, Astrophys. J. **475**, 263 (1997).
[16] R. Monchaux, M. Berhanu, M. Bourgoin, M. Moulin, Ph. Odier, J. -F. Pinton, et al., Phys. Rev. Lett. **98**, 044502 (2007).
[17] M. Rheinhardt and A. Brandenburg, Astron. Nachr. **333**, 80 (2012).
[18] `http://pencil-code.googlecode.com`